TÜBİTAK

Turkish Journal of Earth Sciences

http://journals.tubitak.gov.tr/earth/

Research Article

Turkish J Earth Sci
(2020) 29: 501-520

doi:10.3906/yer-1904-7

Stratigraphy of the Mio-Pleistocene sequence in the Göktepe region based on the fossil record (Muğla, SW Turkey)

Özlem YILMAZ[1,2,*], Talip GÜNGÖR[1], Mine Sezgül KAYSERİ-ÖZER[3], Funda AKGÜN[1], Serdar MAYDA[4], Tanju KAYA[4], Atike NAZİK[5], Yeşim BÜYÜKMERİÇ[6]

[1]Department of Geological Engineering, Faculty of Engineering, Dokuz Eylül University, İzmir, Turkey
[2]Department of Geological Engineering, Faculty of Engineering, Muğla Sıtkı Koçman University, Muğla, Turkey
[3]Institute of Marine Science and Technology, Dokuz Eylül University, İzmir, Turkey
[4]Natural History Museum, Ege University, İzmir, Turkey
[5]Department of Geological Engineering, Faculty of Engineering, Çukurova University, Adana, Turkey
[6]Department of Geological Engineering, Faculty of Engineering, Bülent Ecevit University, Zonguldak, Turkey

Received: 11.04.2019 • **Accepted/Published Online:** 24.12.2019 • **Final Version:** 16.03.2020

Abstract: The sedimentary basins in SW Turkey (e.g., Kale-Tavas, Yatağan, and Ören basins) that developed after the closure of the Neotethys Ocean allow the reconstruction of the tectonic and paleogeographic history of the region. Due to the rich coal reserves, the Yatağan Basin provides a substantial amount of data to infer the paleoenvironment and paleoclimate during the middle Miocene to Pleistocene. Our work provides new paleontological and radiometric data to constrain the age, paleoclimate, and depositional environment of terrestrial deposits of this basin. We present fossil findings such as mammal bones, gastropods, and palynomorph assemblages from the base of the Turgut Formation. According to these fossils, the formation started to deposit in a brackish-freshwater lacustrine environment during the late early Miocene–early middle Miocene interval (MN4–5) under warm, subtropical climatic conditions. The brackish conditions may be explained by a marine transgression in the region. The palynological and paleontological analyses from the lignite and underlying and overlying stratigraphy in the Turgut Formation mark a freshwater environment and warm-temperate climatic conditions during the middle–late middle Miocene (MN6–7). ^{230}Th/U dating results of the uppermost levels of the lacustrine carbonates of the Milet Formation reveal a minimum radiometric age of 346 ± 19 ka BP (middle Pleistocene). The uppermost levels of the Milet Formation overlapped the Göktepe Fault. This may imply continuous subsidence in the basin until ~346 ka.

Key words: Kale-Tavas Basin, Yatağan Basin, palynology, mammals, ostracods

1. Introduction

Extensional basins that develop after the closure of an ocean have a key role in understanding the spatial and temporal evolution from compressional to extensional tectonics. The basins in southwest Turkey are optimal places for studying postcollision events following the closure of the Neotethys Ocean. The development of sedimentary basins, such as the Kale-Tavas, Yatağan, and Ören basins, preserves the evidence of the transition from compression to extension of the regional tectonism (Seyitoğlu et al., 2004, Sözbilir, 2005). These basins in SW Turkey started to develop immediately after the emplacement of the Lycian Nappes over the Menderes Massif (Gürer and Yılmaz, 2002).

The Menderes Massif and the Lycian Nappes are the main tectonic belts of southwest Turkey in the eastern Mediterranean. The Lycian Nappes were emplaced on the Menderes Massif during the Late Cretaceous–Eocene, related to the closure of the northern Neotethys Ocean (Şengör and Yılmaz, 1981; Collins and Robertson, 1998; Yılmaz et al., 2000; Gürer and Yılmaz, 2002; Alçiçek and ten Veen, 2008; Gürer et al., 2013). The boundary of these tectonic belts is unconformably covered by the Oligo-Miocene sequences deposited in the Kale-Tavas Basin (Akgün and Sözbilir, 2001; Gürer and Yılmaz, 2002; Seyitoğlu et al., 2004; Sözbilir, 2005; Gürer et al., 2013). Subsequently, N-S striking normal faults dissected the Kale-Tavas Basin into the Ören and Yatağan basins in the early to middle Miocene (Gürer and Yılmaz, 2002) (Figures 1a).

Most of the previous studies in this area are related to the paleontology, stratigraphy, and/or structural features of the Kale-Tavas, Yatağan, and Ören basins (Becker-Platen 1970; Benda, 1971; Ünal, 1988; Seyitoğlu and Scott, 1991; Yılmaz et al., 2000; Akgün and Sözbilir, 2001; Gürer and

* Correspondence: ozlemyilmaz@mu.edu.tr

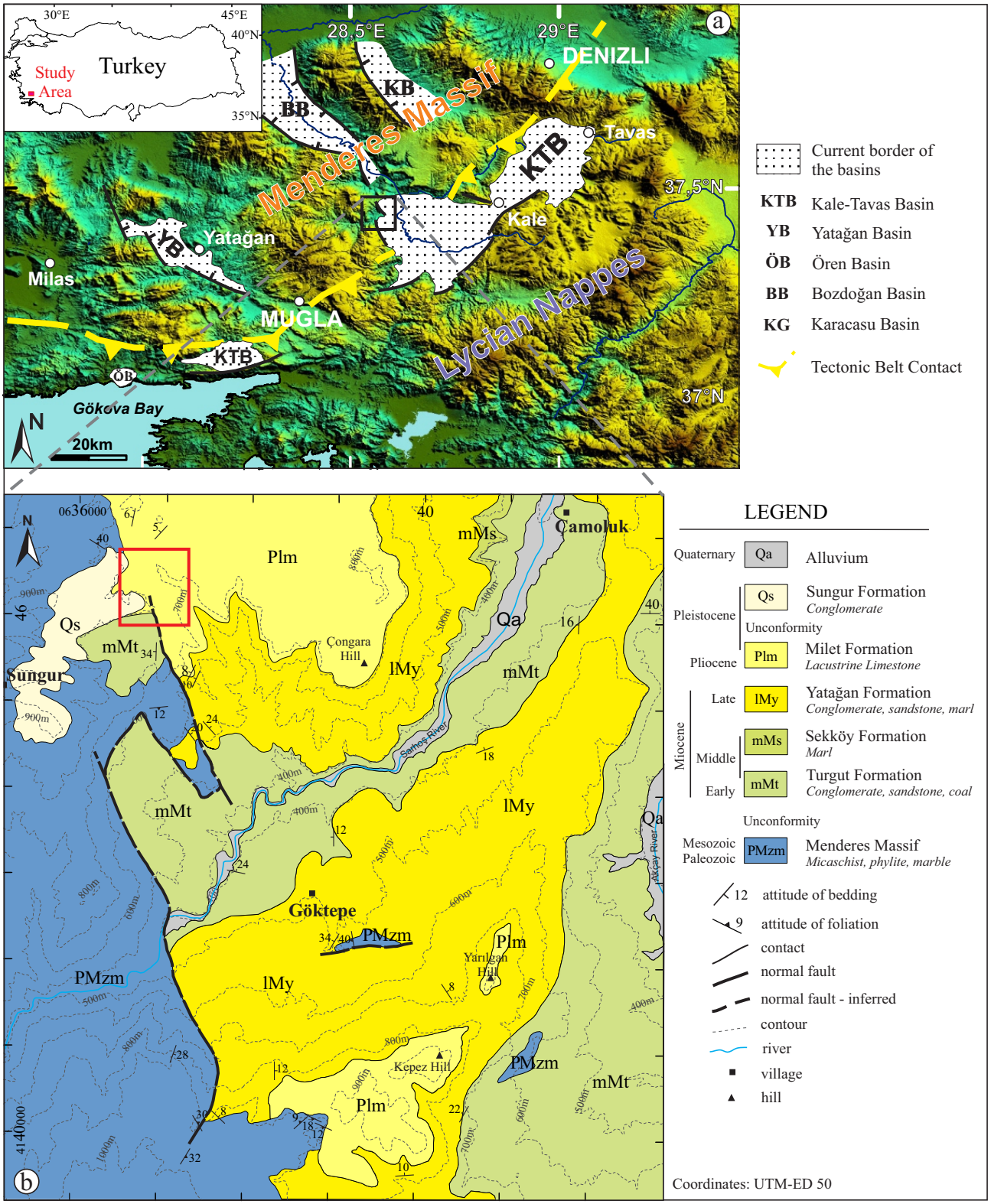

Figure 1. a) Map showing the current geographical position of the Kale-Tavas (KTB), Yatağan (YB), Ören (ÖB), Bozdoğan (BB), and Karacasu (KB) basins. Faults are from Okay (2001), Seyitoğlu et al. (2004), and Ocakoğlu et al. (2014). b) Geological map of the Göktepe area (red square shows the location of Figure 10).

Yılmaz, 2002; Sözbilir, 2005, Özcan et al., 2009, Alçiçek, 2010; Gürer et al., 2013; Kayseri-Özer et al., 2014). These studies have not reached a common explanation yet for the stratigraphy and tectonic evolution of the basins.

The stratigraphy of the Yatağan Basin was documented in detail by Becker-Platen (1970), Atalay (1980), and Hakyemez (1989) (Figure 2). The coal-bearing lacustrine and fluvial deposits in the Yatağan Basin were named as the Muğla Group and divided into the Turgut, Sekköy, Yatağan, and Milet formations from base to top. Due to the rich coal reserves, the Yatağan Basin provides a substantial amount of data to infer the paleoenvironment and paleoclimate during the middle Miocene to Pleistocene. The Turgut, Eskihisar, Bağyaka, Tınaz, and Bayır sectors are the main coal production locations in the Yatağan Basin. These coal deposits were documented in detail by Nebert (1956), Becker-Platen (1970), Benda (1971), Nakoman (1978), Ünal (1988), Seyitoğlu and Scott (1991), Nakoman and İnaner (1996), Querol et al. (1999), and Bouchal et al. (2016, 2017). These studies were focused on coal geology, coal quality, or coal reserve estimation. Some others are related to the sporomorph contents of the coal layers. Nevertheless, the stratigraphic position of the lignite beds is still under debate. Atalay (1980) suggested that the Turgut Formation can be differentiated from the Sekköy Formation with thick coal layers. Bouchal et al. (2016, 2017) confirmed the same stratigraphic position of coal layers described by Atalay (1980). However, Querol et al. (1999) and Inaner et al. (2008) put this main coal seam within the Sekköy Formation.

In this paper, we describe the paleontology and stratigraphy of the Mio-Pleistocene sequence in the Göktepe area. The area is located in the west of the Kale-Tavas Basin, in the south of the Bozdoğan Basin, and is currently separated by a mountain range from the Yatağan Basin (Figure 1a). We present new paleontological and radiometric data that reveal the depositional environment and paleoclimatic conditions of the region. We describe palynomorph assemblages, gastropods, ostracods, and mammalian fossils that allow us to constrain the new age of the Turgut Formation. In addition, we provide the U series dating radiometric age for the Milet Formation. Based on our new data, we discuss the stratigraphy and tectonic history of the Göktepe area.

2. Materials and methods

We studied the basin-fills throughout detailed geological mapping at 1/25,000 scale and measured sections from the two different outcrops of the Turgut Formation. Pollen assemblages (palynomorphs), ostracods, gastropods, and mammal bones and teeth have been collected from the lignite layers and surrounding clay levels of the Turgut Formation. We also applied U series dating for the travertines of the Milet Formation that were sampled from a travertine quarry at the Kepez Hill.

2.1. Paleontological analysis

We studied the pollen assemblages of five samples from the Sungur location and 38 samples from the lignite seams, which were collected from 100 m below the surface in a coal mine and from the drilling cores around Çamoluk village. The pollen analyses were performed at Dokuz Eylül University, İzmir, Turkey, using standard palynological techniques (e.g., Batten, 1999). We treated the samples with HCl and HF to remove the carbonates and silicate minerals, respectively. The separation of the palynomorphs was performed by centrifugal action, using $ZnCl_2$ as a heavy liquid.

The ostracod analyses were performed at Çukurova University, Adana, Turkey. Claystone samples of 100 g were disaggregated with 10% H_2O_2 and stored for 24 h. The samples were then washed with pressurized water through 100- and 150-mm mesh sieves and dried at 50 °C. The ostracod contents of residue materials were examined with a binocular microscope. Scanning electron microscope (SEM) images were taken at Muğla Sıtkı Koçman University on a JSM 7600F field emission scanning electron microscope (JEOL, Japan) at an accelerating voltage of 15 kV. The ostracod samples were placed on specimen stubs with double-sided adhesive carbon tape and were coated with gold (Emmitech K550, UK).

The gastropods and the mammal bones were studied at Zonguldak Bülent Ecevit University, Zonguldak, Turkey, and the Ege University Natural History Museum (EUNHM), Bornova, İzmir, Turkey respectively.

2.2. U series dating

U series dating was applied to eight micritic, nonporous samples from travertine deposits of the Milet Formation. The analysis was performed at the GEOTOP Research Center of the University of Quebec in Montreal, Canada. The details of the analytical procedure were described by Ghaleb et al. (2019). Briefly, about 1 g of travertine sample was cut using a rotary tool with a diamond disc (Deremel). Then the subsamples were weighed in Teflon beakers, in which an accurately weighed amount of ^{236}U-^{233}U-^{229}Th spike was evaporated at low temperature (~60 °C) to determine U and Th isotopes by isotope dilution technique. The samples were covered with deionized water and dissolved slowly by adding HNO_3 (7 M) drop by drop. After the total dissolution, about 10 mg of the iron carrier was added and the samples were left overnight in order to ensure spike-sample equilibration. U and Th isotopes were coprecipitated with $Fe(OH)_3$ by adding ammonium hydroxide to the solution until pH 8–9 was reached. The precipitates were recovered by centrifugation, washed with water, and dissolved in HCl (6 M). Chemical separation of U and Th isotopes was done by anion exchange resin

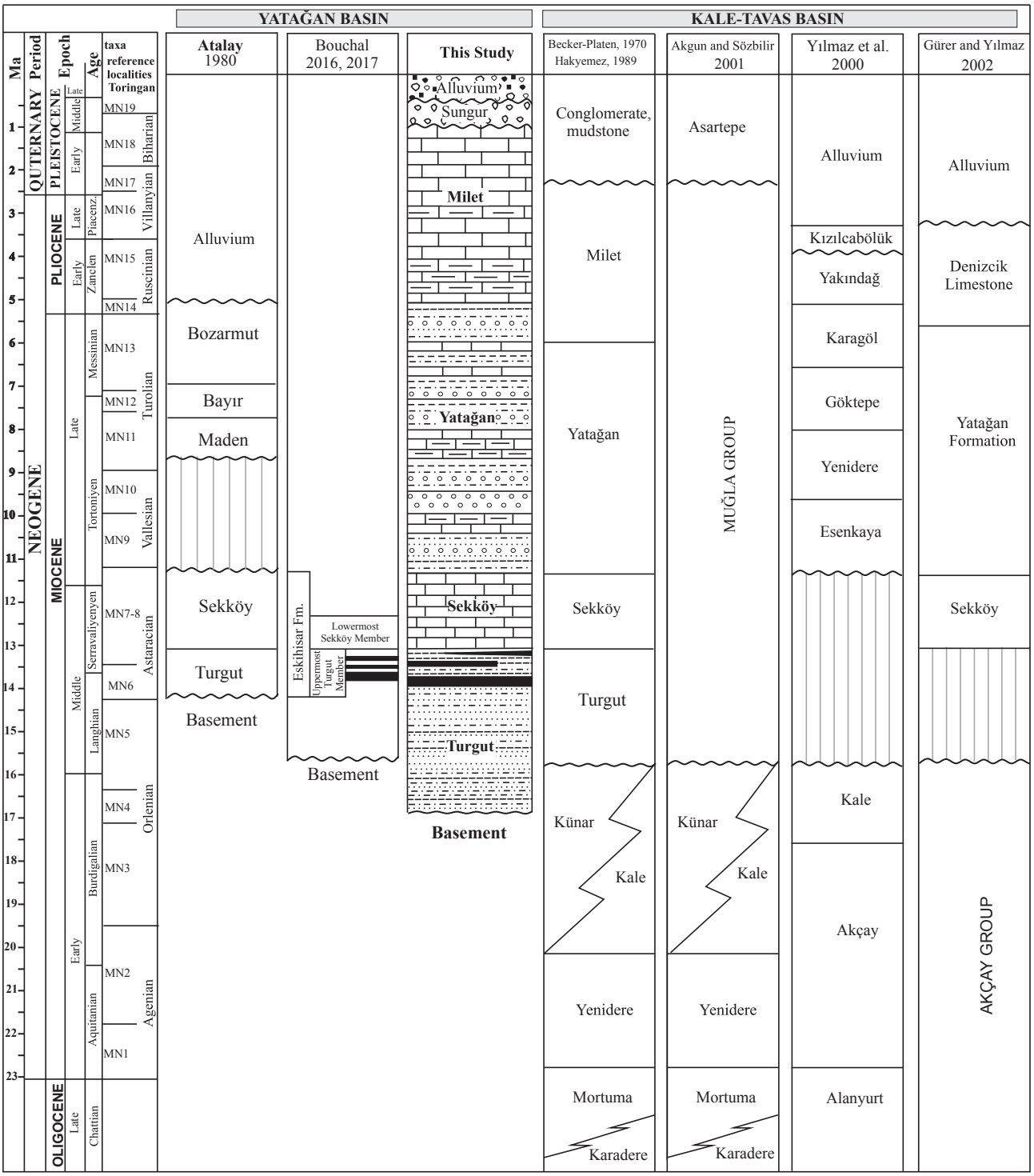

Figure 2. Stratigraphy of the Yatağan and Kale-Tavas basins in previous and present studies.

(AG1X8, 200–400 mesh). Thorium fractions were recovered with HCl (6 M) while the uranium with iron fractions were eluted with water. Finally, U purification from iron was done using U-Teva resin, the iron being eluted with HNO_3 (3 M) and the uranium with HNO_3 (0.02 M). For the thorium fraction, after evaporation, a purification column of 2 mL of AG1X8 was used in HNO_3 (7 M) and eluted with HCl (6 M).

Measurements of U and Th isotopes were performed using a Nu Instruments Multi-Collector via inductively

coupled plasma mass spectrometry (MC-ICP-MS). The ^{236}U-^{233}U certified ratio of the spike was used to correct for mass bias for U and Th isotopes. Age calculations and detrital corrections were done using the Isoplot 4.15 software program (Ludwig, 2012).

3. Stratigraphy

3.1. Basement rocks

Metamorphic rocks of the Menderes Massif form the basement and extend throughout the west of the study area (Figure 1b). The Lycian Nappes are not exposed at Göktepe, but they are found around the villages of Yeşimendere and Özlüce, near Muğla.

The Menderes Massif starts with the fusulinid-bearing Permo-Carboniferous Göktepe Formation (Önay, 1949; Erdoğan and Güngör, 2004). The formation is made up of dark brown to gray phyllites, schists, quartzites, and marbles. Calc schist-chlorite schist intercalations with rare quartzite interlayers show a strong brittle deformation. Foliations are thin and have a shallow dip angle. The Göktepe Formation is unconformably overlain by a Mesozoic succession of marbles (Önay, 1949; Konak et al., 1987; Özer and Sözbilir, 2003; Erdoğan and Güngör, 2004). In the study area, the Mesozoic sequence is composed of white to dark gray marbles and black marbles. The marbles show a prominent foliation with varying dip directions.

3.2. Mio-Pleistocene basin-fill succession

3.2.1. Turgut Formation

The unconformable Mio-Pleistocene sequence starts with the Turgut Formation (Figures 2 and 3). The Turgut Formation crops out at the lower elevations of the study area, particularly along both sides of the Sarhoş Stream and Akçay River (Figure 1b). The Turgut Formation is made up of yellowish-gray and green, thin- to medium-bedded claystone, mudstone, sandstone, and conglomerate alternations including some thin limestone levels (Figures 4a and 4b). Conglomerate levels contain small-scale channel fills. Sandstones show mostly cross-bedding (Figure 4b).

The lower part of the formation is exposed in a small area near Sungur village (Figures 1b and 5a). The detailed section of this outcrop is given in Figure 5b. The section starts with yellowish-orange, laminated, marl-mudstone, very thin pale green claystone and thin laminated brownish mudstone. The section continues upwards with yellowish beige mudstone, gray claystone, and siltstone. The upper levels of the section are composed of gray-colored, poorly lithified, medium- to coarse-grained sandstones and matrix-supported granule- and pebble-sized conglomerates. The sandstones and conglomerate levels show both parallel and cross-bedding. The section ends with sandstones >10 m thick. Abundant broken gastropod shells, bivalve fossils, and mammal bones are found in this outcrop (Figures 5c, 5d, and 5e). These mammal bones and gastropods have been collected and the claystone levels were also sampled for palynological analysis (Figure 5f). The fossil records give the age of late early–early middle Miocene. The details are given in Section 4.

The upper parts of the formation are made up of claystone, limey claystone, and clayey limestone alternations (Figures 6a–6f). To the north of Çamoluk village, this alternation includes two seams of lignite (Figures 6a and 6c). The thickness of the lignite seams varies along its strike and wedges out. The main lignite seam is approximately 2 m thick and contains mammal bones and teeth. This lignite layer grades upward into beige-colored, laminated claystone and dark green claystone with abundant broken gastropod shells and ostracod fossils (Figure 6b). Dark green claystone levels include some plant remnants. On top of this layer, there are gray-beige, clayey limestone and beige claystone levels with broken gastropod shells and abundant ostracods. The above-lying second seam has been measured from drilling cores and is approximately 30 cm thick (Figure 6c). These coal seams and surrounding clay levels were sampled for palynological analysis and gastropods, ostracods, and mammal bones have been collected from these layers. The fossil record gives the age of middle–late middle Miocene. The details are given in Section 4.

The Turgut Formation is conformably overlain by the Sekköy Formation (Atalay, 1980; Hakyemez, 1989).

3.2.2. Sekköy Formation

The Sekköy Formation is poorly exposed in the west of Çamoluk village with elevations of approximately 400 m (Figure 1b). The formation is composed of gastropod-bearing, lacustrine clayey limestones. There are no lignite layers observed. The lignite layers are located in the upper part of the Turgut Formation and these coal layers gradationally pass upward to the lacustrine deposits of the Sekköy Formation (Figure 6a).

The age of the formation is late middle Miocene (Atalay, 1980). The Sekköy Formation is conformably overlain by the Yatağan Formation (Figure 3).

3.2.3. Yatağan Formation

The Yatağan Formation crops out along the hillslopes of the Çongara, Yarılgan, and Kepez hills, at elevations of above ~400 m (Figure 1b). This formation has a distinct orange-red color and is composed of conglomerate, sandstone, siltstone, and mudstone alternation with some clayey limestone and limestone lenses (Figure 7). The formation starts with matrix-supported, poorly sorted conglomerates. These conglomerates contain subrounded, subangular clasts and alternate with medium- to coarse-grained cross-bedded sandstones. These fluvial clastics change upwards to lacustrine limestone beds.

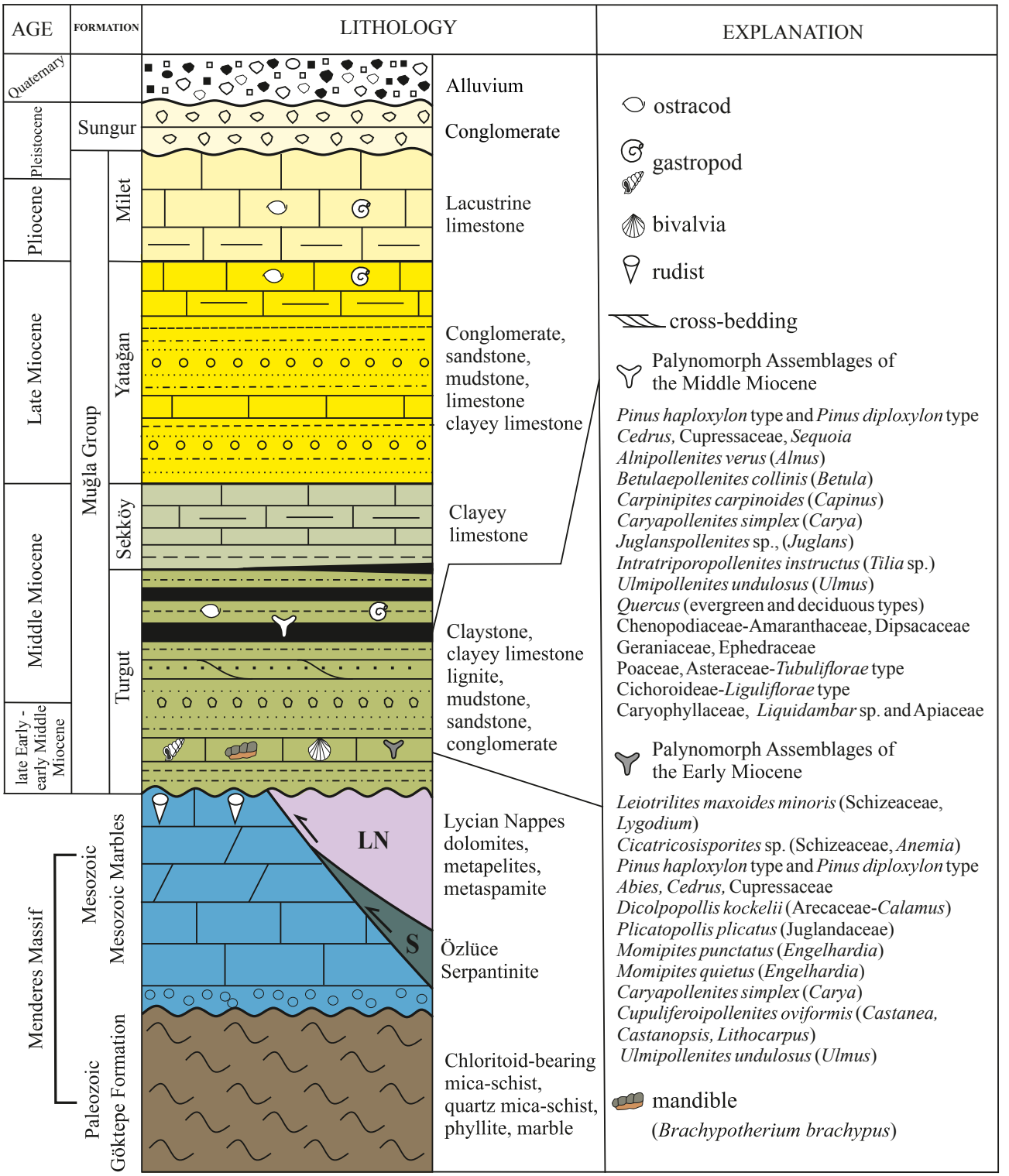

Figure 3. Stratigraphic section of the Göktepe area (modified after Atalay, 1980 and Hakyemez, 1989). Mio-Pleistocene sedimentary sequence covers the tectonic boundary of the Menderes Massif and Lycian Nappes along an angular unconformity.

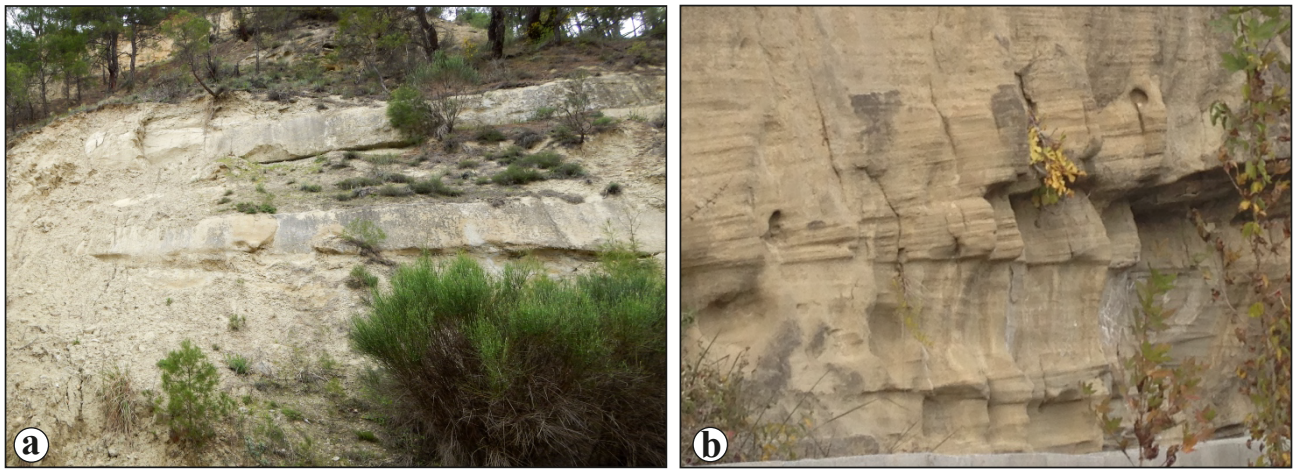

Figure 4. Field views of the Turgut Formation (640920 E, 4146200 N). a) Field photographs showing gray beige-colored Turgut Formation. The formation is composed of mudstone, sandstone, and conglomerate (including max. pebble-sized grains) alternation. b) This photo shows the cross-bedding structures in the thickly bedded sandstones.

The age of the Yatağan Formation is Turolian (upper Miocene) based on vertebrate fossils described by Atalay (1980) and Hakyemez (1989). The Yatağan Formation is conformably overlain by the Milet Formation.

3.2.4. Milet Formation

The Milet Formation was described by Becker-Platen (1970) as the Milet beds and revised by Hakyemez (1989) to the Milet Formation (Figure 2). In the study area and further east towards the town of Kale (Denizli), the Milet Formation is exposed on top of plateaus around Göktepe village (Figure 8). The Milet Formation is composed of yellowish cream claystone, marl, and travertine-type lacustrine limestones. The lower parts of the formation are graded vertically into the orange-colored conglomerates of the Yatağan Formation and pass through upward travertine-type lacustrine limestones. The thickness of the travertine is approximately 80 m and it includes plant remains and gastropod and ostracod fossils. The Milet Formation is almost horizontal in the south of the study area, but it shallowly dips to the NW (5–10°) north of Göktepe village.

Atalay (1980) determined the age of the Milet Formation as upper Miocene (Turolian)–Pliocene according to vertebrate fossils from Bozarmut village (Muğla). Hakyemez (1989) also stated the age of the formation as Pliocene because stratigraphically the Milet Formation lies on top of sequences that contain Turolian mammal fossils. In this study, U series dating was used to determine the age of the travertine-type lacustrine limestones of the Milet Formation at the uppermost part of the formation. These results were first presented by Yılmaz et al. (2016). The radiometric dating results show a Middle Pleistocene age for the travertines. The details are given in Section 4.

The Milet Formation is unconformably overlain by the Sungur Formation.

3.2.5. Sungur Formation

The Sungur Formation is exposed in a small area between Göktepe and Sungur villages (Figure 1b). The Sungur Formation consists of brownish-red, matrix-supported, very poorly sorted, poorly lithified conglomerates and sandstones (Figure 9). Conglomerates are made up of angular pebble- and cobble-sized clasts of schist and marble. The matrix is composed of fine-grained sand and silt.

The alluviums of the Akçay and Sarhoş rivers are the Quaternary deposits of the study area that unconformably overlay the sequence (Figures 1b and 3).

4. Results and discussion

4.1. Late Early Miocene–Early Middle Miocene

The Turgut Formation is exposed along a road-cut outcrop and a drainage channel near Sungur village (Figures 1b and 5a). We collected mammal bones and gastropods from this outcrop. In addition to these fossils, five claystone samples were also taken for palynological analysis. Fossil contents of this formation are given below.

4.1.1. Gastropods

Although the taxonomic revision of *Tinnyea laurea* s.s. is not complete (syn. *Tinnyea escheri* Brongniart, 1822; Harzhauser et al., 2016), we found species that resemble *Tinnyea laurea* (Matheron, 1843) in having opisthocline axial ribs (Figure 5d). The thiarid *Tinnyea* is an extinct freshwater genus, common in the Oligocene-Neogene lake systems of Mediterranean and Paratethys areas (Harzhauser and Mandic, 2008; Harzhauser et al., 2016). *T. escheri* s.l. is a characteristic taxon for freshwater to

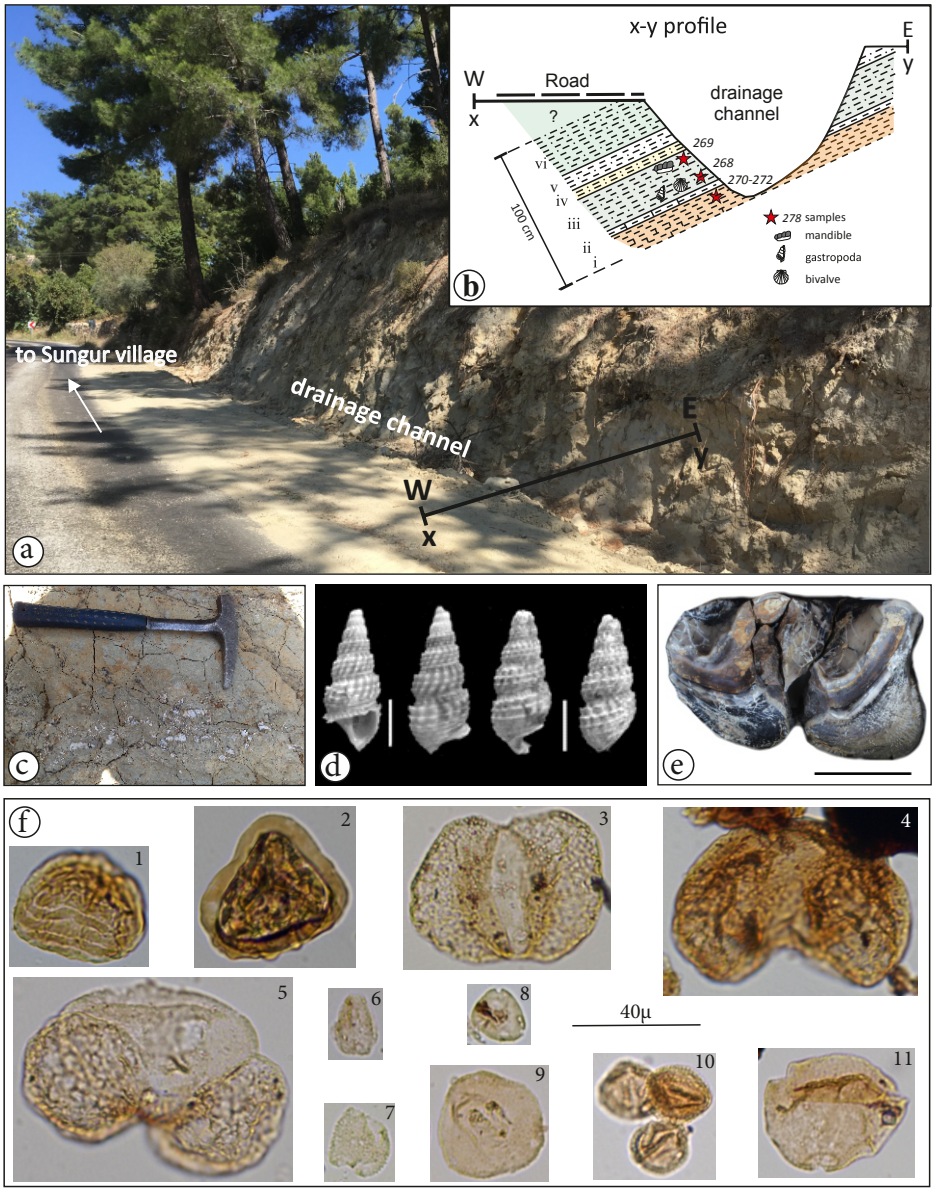

Figure 5. The lower parts of the Turgut Formation crops out in a narrow zone (0636632 E, 4145695 N). a) The fossil location on the Göktepe-Sungur road. b) Cross-section that gives detailed stratigraphy (i. yellowish, thin laminated, carbonated claystone, mudstone; ii. carbonated claystone; iii. green, fractured claystone with broken gastropod shells and branches, and thin laminated brownish mudstone at lower levels; iv. yellowish-gray mudstone; v. white claystone, siltstone; and vi. greenish-gray, weekly bounded sandstone). c) Bivalve and gastropod shells in claystone levels. d) SEM photos of gastropods. e) Left lower m1 of *Brachypotherium brachypus*, scale: 2 cm. f) Palynological samples (1. Schizaeceae, 2. Polypodiaceae, 3. *Cathaya*, 4. *Cedrus*, 5. *Pinus silvestris* type, 6. and 7. *Calamus*, 8. *Engelhardia*, 9. *Carya*, 10. Adoxaceae-*Viburnum*, 11. *Fagus*).

brackish environments and commonly observed in Thrace and Central Paratethyan basins (Mikuz and Pavsic, 2000; Harzhauser et al., 2002, 2011, 2016). Thus, our record can be considered indicative of similar environments.

4.1.2. Mammalian records

The Sungur locality yielded a rhino mandible fragment referred to *Brachypotherium brachypus* (Figure 5e). The material is biometrically larger than *Brachypotherium brachypus* remains from the middle Miocene locality of Paşalar (NW Turkey) (Fortelius, 1990) as well as those from European ones. It is also larger than *B. minor* records from Africa (Geraads and Miller, 2013) and *B. perimense* from middle-late Miocene localities of Siwalik, Pakistan. Furthermore, it is quite smaller than *B. goldfussi*

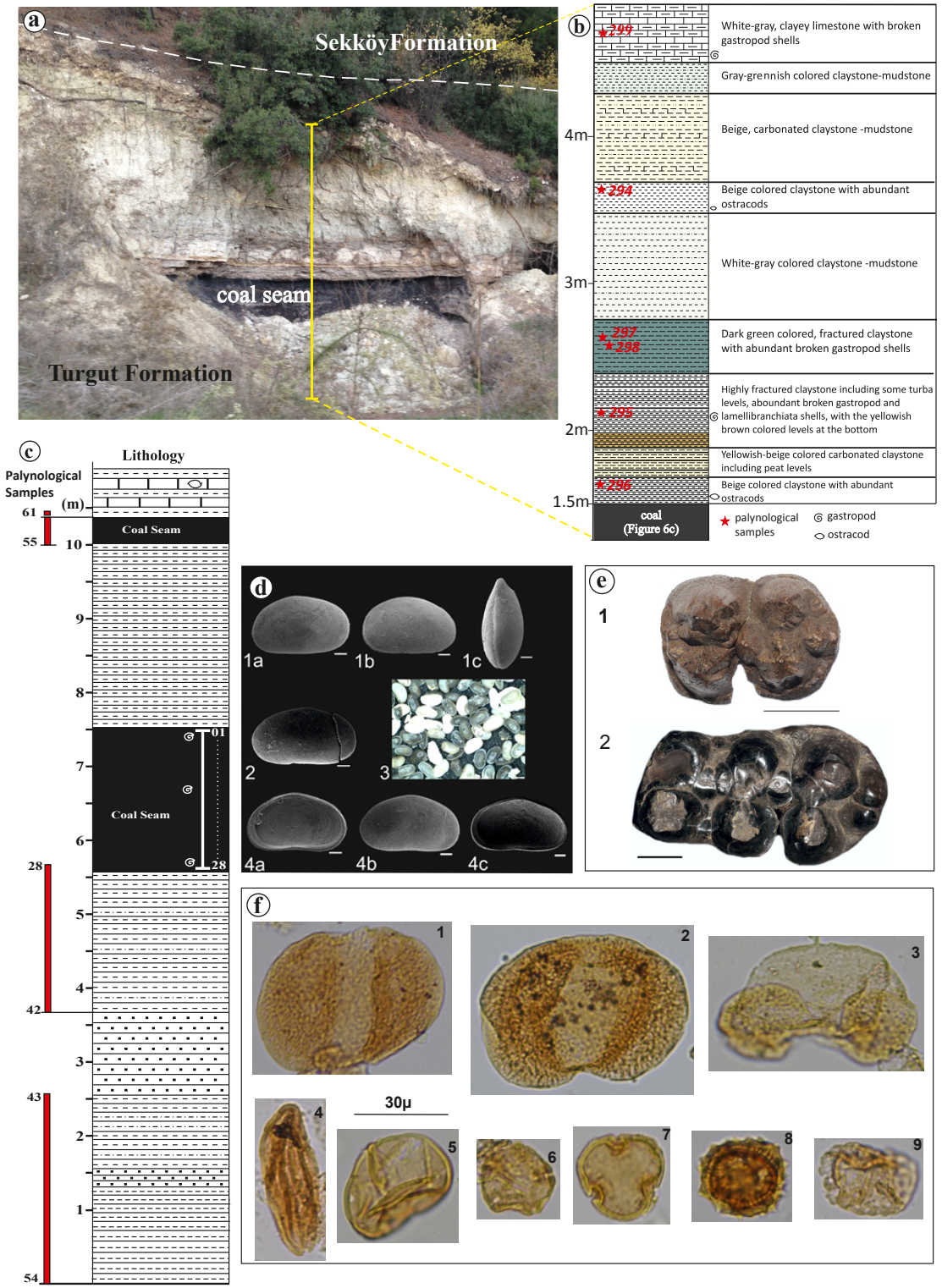

Figure 6. a) Field view of the coal-bearing levels of the Turgut Formation (0641305 E, 4147993 N). b) Type section of the upper levels of the Turgut Formation. c) Compiled measured section of the long-wall face in the tunnel and drilling logs of the coal-bearing layers of the Turgut Formation. d. Ostracod images (1. *Heterocypris formalis* (Mandelstam), 1a. external view of the left valve, 1b. external view of carapace, 1c. dorsal view of carapace. 2. *Heterocypris* ex gr. *gregaria* (Skoksberg), external view of the right valve. 3. Stereomicroscope image of ostracod assemblage. 4. *Heterocypris salina* (Brady), 4a and 4c. internal view of the right valve, 4b. external view of the right valve. e) Fossil mammal teeth (1, right lower m2 of *Gomphotherium angustidens*; 2. right lower m2 of *Megalocherus homon*gus; scale: 2 cm). f. Palynomorph assemblages (1. *Cathaya*, 2. *Cedrus*, 3. *Pinus silvestris* type, 4. Ephedraceae, 5. *Carya*, 6. *Alnus*, 7. *Tilia*, 8. Asteraceae-Asteroideae type, 9. Chenopodiaceae).

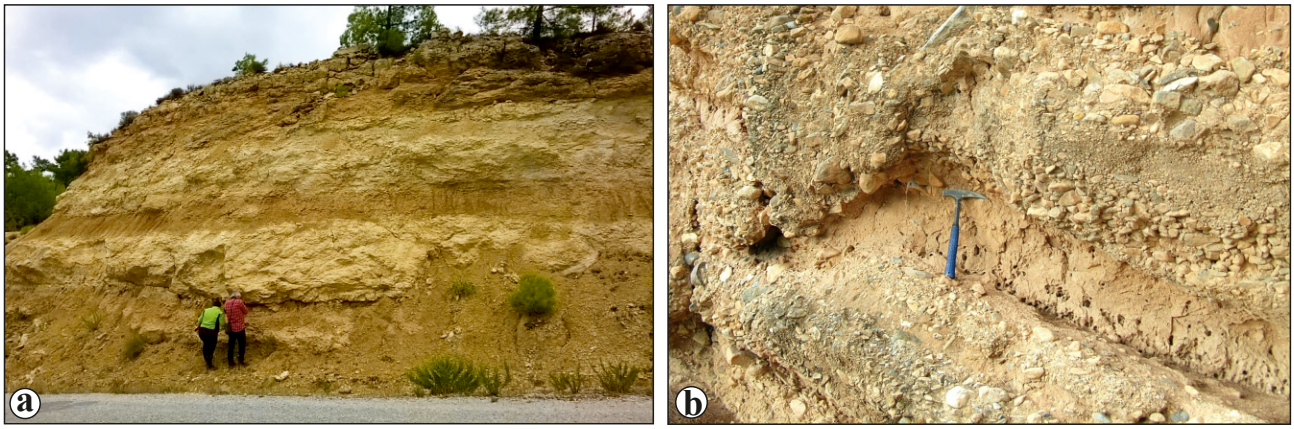

Figure 7. Field photographs of the different lithologies of the Yatağan Formation (0641170 E, 4143241 N). a) View of the fine-grained levels of the formation that are made up of fluvial deposits, consisting of silt, sand, clay, and marl alternations (outcrop height is approx. 11m). b) Orange-colored conglomerate levels of the formation.

Figure 8. Field photographs of the Milet Formation (Kepez Hill). a) Field view from Kepez Hill to Göktepe village. b and c) Travertine-type lacustrine carbonates of the Milet Formation. Triangles show the sample locations for U series dating (samples 7 and 8 were taken from the benches at lower levels).

Figure 9. Field views of the Sungur Formation. a) The formation has an orange color and horizontal beds. b) The formation is composed of poorly sorted conglomerate including angular grains of Menderes metamorphics in a sandy matrix.

from Eppelsheim (MN6–9). The Sungur specimen is morphologically and metrically similar to those from the early middle Miocene (MN5) locality of Kultak (Muğla, Turkey) (Kayseri-Özer et al., 2014).

4.1.3. Sungur palynomorph assemblage

The microflora of sedimentary sequences in the lower part of the Turgut Formation is characterized by spores of Pteridophyta (*Verrucatosporites* sp., 1%; *Leiotrilites maxoides minoris* (Schizeaceae, *Lygodium*, 1%), *Polypodiaceoisporites* sp. (Pteridaceae, *Pteris*), *Cicatricosisporites* sp. (Schizeaceae, *Anemia*, 1%–4%), *Laevigatosporites* sp., and *Echinatisporis* sp. (*Selaginella*, 1%)). Abundance and variety of the gymnosperms (>50%; Cupressaceae, *Cathaya*, *Abies*, *Cedrus*, and Pinaceae-*Pinus haploxylon* and *diploxylon* types) in this assemblage indicate the existence of middle and high altitude landscapes around the deposition area. We also identified *Dicolpopollis kockelii* (Arecaceae-*Calamus*, 1%–2%), which is a species of the *Calamus* palm family marking tropical and subtropical areas. This genus is also observed in Oligocene-early Miocene sedimentary rocks in Turkey (e.g., Nakoman, 1966; Akyol, 1971; Ediger et al., 1990; Akgün and Sözbilir, 2001; Sancay et al., 2006; Akgün et al., 2007, 2013; Batı and Sancay, 2007; Kayseri, 2010; Akkiraz et al., 2011; Kayseri-Özer et al., 2014). *Plicatopollis plicatus* (Juglandaceae) is another palynostratigraphically important species in the Anatolian and European palynofloras and its abundance decreases from the Eocene to Miocene (e.g., Akgün et al., 2007, 2013; Akkiraz et al., 2011; Kayseri-Özer, 2014). In this study, *Dicolpopollis kockelii* and *Plicatopollis plicatus* are less abundantly recorded in the samples of the lower part of the Turgut Formation. In addition, some angiosperm species such as *Momipites punctatus* (*Engelhardia*, 1%–4%), *M. quietus* (*Engelhardia*, 1%), *Caryapollenites simplex* (*Carya*, 1%), *Cupuliferoipollenites oviformis* (*Castanea*, *Castanopsis*, *Lithocarpus*, 1%), *Ulmipollenites undulosus* (*Ulmus*, 1%), *Triporopollenites coryloides* (*Corylus*, 1%), *Faguspollenites verus* (*Fagus*, 1%), *Faguspollenites* spp. (*Fagus*, 1%), *Caprifoliipites viburnoides* (Adoxaceae, *Viburnum*, 26%), *Quercoidites* spp. (*Quercus*, 1%), *Acaciapollenites* sp. (*Acacia*, 1%), and *Tricolporopollenites* sp. (*Lonicera*, 1%) are also recorded in the Sungur palynoflora (Figure 5f). According to this palynofloral composition, the deposition period of the formation is from the Burdigalian to Langhian. The age constraints obtained from palynological findings are coherent with the ages obtained from the mammalian fossils (MN4–5). Palynological findings further show that the formation was deposited in a lacustrine environment under warm subtropical climatic conditions. Spores and pollen species (*Acrostichum aureum*, *Anemia*, *Nypa*, *Pelliciera*, *Acacia*, *Rhizophora*, *Avicennia*, and *Calamus* palm) and palynomorphs (e.g., *Botroyococcus*, microforaminiferal linings, and dinoflagellate species) prefer to live in mangrove and back-mangrove paleoenvironments that have brackish conditions due to marine influences (e.g., Gruas-Cavagnetto, 1977; Cavagnetto and Anadón, 1996; Riegel et al., 1999; Plaziat et al., 2001; Akgün, 2002; Akgün et al., 2002; Akkiraz et al., 2008; Kayseri-Özer, 2014). In this study, the existence of palynomorphs in the Sungur palynoflora such as *Botroyococcus*, *Acaciapollenites*, *Dicolpopollis*, and *Cicatricosisporites* that can tolerate brackish conditions implies that this may be a brackish lake.

4.2. Middle–Late Middle Miocene

We collected two samples (samples 294 and 295) for ostracod analysis and four samples (samples 296–299) for

palynomorph analysis from the limy claystone and clayey limestone levels of the Turgut Formation around Çamoluk village (Figure 6b). In addition, we sampled the 2-m-thick coal layer from 100 m below the earth's surface, along the long-wall face in the underground coal mine. The second thin coal seam and the other clay levels were sampled from the drilling cores (Figure 6c). These samples were used for the analysis of palynomorph assemblage and mammalian fossils. The fossil findings are described below.

4.2.1. Ostracods

The species of the genus *Heterocypris* were found in samples 294 and 295 (Figures 6b and 6d). These are as follows: *Heterocypris formalis* (Mandelstam) (Miocene-Pliocene) (Serbia, China, Turkey), *Heterocypris* ex gr. *gregaria* (Skoksberg) (middle Miocene-Pliocene) (Turkey), and *Heterocypris salina* (Brady) (late Miocene-Recent) (Slovakia, Turkey, Romania, Bulgaria, Greek islands, and Iran). Most species of *Heterocypris* are common in freshwater environments, while some prefer oligo- to mesohaline habitats (van Morkhoven, 1963). These populations are characteristic for limnic environments (Freels, 1980; Witt, 2003; Matzke-Karasz and Witt, 2005).

4.2.2. Mammalian records

Despite the small number of specimens, mammal remnants were extremely well preserved. We recorded dental remains of two proboscidean taxa at Çamoluk: a fragmentary astragal of a primitive equid, *Anchitherium* sp., and a single lower molar of a giant suid. For proboscideans, a lower second molar and a portion of an upper tusk can be referred to *Gomphotherium angustidens*, which is the most common gomphothere of Europe during the middle Miocene (Figure 6e, inset 1). Some additional molar fragments that we found also display the typical morphology of this taxon. This species is known from Anatolia, mainly from the early middle Miocene localities of Bursa-Paşalar (MN5–6), Muğla-Kultak (MN5), and late middle Miocene localities of Muğla-Sarıçay and Çatakbağyaka (MN7/8). Metrically, *G. angustidens* from Çamoluk falls in the size range of *G. angustidens* from the middle Miocene (Astaracian, MN6–8) localities of France and Germany and it is larger than the Paşalar samples, though these taxa did not show a tendency towards increasing molar size over time (Tassy, 2014). However, the well-developed posterior cingulum and bunodonty clearly differentiate the Çamoluk specimens from the Orleanian (MN4–5) forms, such as at Corcoles (Spain, MN4) and Quinta Grande (Portugal, MN4) (Bergounioux et al., 1953; Mazo, 1977, 1996; Maldonado et al., 1983; Tassy, 1985). The occurrence of a second proboscidean species at Çamoluk is supported by an upper second molar. This specimen is tentatively referred to the amebelodontid genus *Protanancus* based on its generally well-pronounced pseudo-anancoidy, cementodonty, and posttrite conules. Besides the Anatolian records from the middle Miocene localities, such as İzmir-Mordoğan, Bursa-Paşalar, and Ankara-Çandır, the Çamoluk specimen mostly resembles the *Protanancus* material from Bulgaria-Vetren, which was also dated to the middle Miocene (Markov and Vergiev, 2010).

A second lower molar represents a giant Kubanochoerine suid and confirms the presence of the enigmatic genus *Megalochoerus* at Çamoluk. The kubanochoerines migrated into Eurasia during MN5 and survived until MN7/8 (Pickford, 2001). The previous record from Turkey, an upper molar from Ankara-Kazan-İnönü (MN6), was thought to be an M2 of *Kubanochoerus mancharensis* (junior synonym of *Megalochoerus humungous*) (Pickford and Ertürk, 1979; van der Made, 1996) (Figure 6e, inset 2). Since the Kubanochoerine suids underwent a rapid increase in size from early to middle Miocene times, they can be used for biochronology (Pickford, 2001; Pickford and Morales, 2003). In light of this, the Çamoluk specimen fits well with the morphologic and metrical features of the Astaracian species *M. humungous*, although it has slightly lower range values compared to the youngest records of this taxa, collected from MN8 localities (late Astaracian) of Pakistan. This could also be interpreted as a sign of an older age than MN8 for Çamoluk. The fragmentary astragal of anchithere remains from Çamoluk is morphologically identical to the Turkish and European middle Miocene *Anchitherium* samples but distinguished from the early Miocene forms by its relatively larger size.

4.2.3. Çamoluk palynomorph assemblage

Palynological data were obtained from 38 samples of coal and claystone levels of the Turgut Formation (Figures 6c and 6f). Spores are various and less abundant, except for *Laevigatisporites haardti* (Pteridophyta). Also, gymnosperm pollen (Pinaceae, *Pinus haploxylon* and *diploxylon* types, *Cathaya* sp., *Glyptostrobus/Taxodium/Cryptomeria* sp., *Podocarpus* sp., *Cedrus* sp., *Sequoia* sp., and Cupressaceae, 5%–60%) are more abundantly recorded in all samples. The woody angiosperm plants are represented by *Alnipollenites verus* (*Alnus*, 1%–3%), *Betulaepollenites collinis* (*Betula*, 1%), *Carpinipites carpinoides* (*Capinus*, 1%), *Caryapollenites simplex* (*Carya*, 1%–5%), *Juglanspollenites* sp. (*Juglans*, 1%), *Intratriporopollenites instructus* (*Tilia*, 1%), *Ulmipollenites undulosus* (*Ulmus*, 1%–2%), and *Quercus* evergreen and deciduous types, 1%–3%, and *Caprifoliipites sambucoides* (Adoxaceae-*Sambucus*, 1%), *Lonicerapollis* sp. (*Caprifoliaceae-Lonicera* sp., 1%), *Faguspollenites verus* (Fagaceae-*Fagus*, 1%), and *Aceripollenites* sp. (*Acer*, 1%). In contrast to the lower part of the Turgut Formation, herbaceous angiosperm pollen (e.g., Chenopodiaceae-Amaranthaceae, Dipsacaceae, Geraniaceae, Ephedraceae, Poaceae, Asteraceae-Tubuliflorae type, Cichoroideae-

Liguliflorae type, Caryophyllaceae, *Liquidambar* sp., and Apiaceae, 5%–10%) are various and abundant in the Çamoluk palynoflora. This palynomorph association of the Turgut Formation resembles the middle-late middle Miocene palynomorphs associations recorded in other sites of Anatolia (e.g., Kırşehir, (Akgün et al., 1995), Büyük Menderes Graben (Akgün and Akyol, 1999); Konya-Ilgın (Karayiğit et al., 1999), Soma (Erdei et al., 2002), Western Anatolia (Akgün et al., 2007), and Çorum and Sivas (Kayseri and Akgün, 2008)). Based on our palynofloral data, the Turgut Formation was deposited under a warm temperate climate during the middle-late middle Miocene (Akgün et al., 2007; Kayseri-Özer et al., 2014).

4.3. Middle Pleistocene

4.3.1. U series dating

U series analysis was carried out with eight hand samples that were taken from a travertine quarry located on Kepez Hill (Figure 1b and 8a–8c). This quarry has several benches that cut an 80-m-thick horizontal travertine sequence (Figures 8b and 8c). Eight micritic and nonporous samples were collected from the benches. The results are given in the Table.

The basis of U series dating is that the $CaCO_3$ phase incorporates only uranium (soluble in oxidizing conditions) and not ^{230}Th (insoluble) during the precipitation. The uranium then produces the authigenic ^{230}Th by radioactive decay and the activity ratio of ^{230}Th/U increases from zero at the time of precipitation until reaching the secular equilibrium value around 500–600 ka. If the radioactive system remains closed (no loss or gain of any U and Th isotopes except by radioactivity), then the activity ratio of ^{230}Th/U allows calculation of the time since the precipitation of the carbonate phases.

Stratigraphically, the ages of our samples taken from the uppermost levels of the sequence must be younger than those from the bottom. However, the results are incompatible with the stratigraphy (Table). There may be several potential reasons for this inversion in the stratigraphic order. The first one is that our travertine samples have incorporated variable amounts of detrital contamination. This is indicated by the presence of variable amounts of ^{232}Th (and all other thorium isotopes). In such a case, the measured ^{230}Th in our samples corresponds to the sum of authigenic ^{230}Th that is produced by incorporation with both uranium and the nonauthigenic ^{230}Th related to detrital contamination. Thus, we should subtract the amount of detrital ^{230}Th from the total ^{230}Th before calculating the age of a sample. We used an average crustal correction model similar to the one used by Ludwig and Paces (2002) to obtain the corrected ages that are given in the Table. Specifically, ^{232}Th was used as an index and typical crustal Th/U was used for the detrital component. The activity ratio values used are ^{232}Th/^{238}U = 1.21 ± 50%, ^{230}Th/^{238}U = 1 ± 10%, and ^{234}U/^{238}U = 1 ± 10%. We believe that with such assigned errors for the detritus component the detrital correction should correct our sample results in a manner that covers most of the natural detritus observed on the earth's surface. As seen in the Table, the corrected ages are still not compatible with the stratigraphic order, therefore indicating that detrital contamination is not the primary cause for the incompatibility with the stratigraphic order and another process should be evoked. As mentioned above, U series dating is based on the assumption of a closed radioactive system (no loss or gain of any U and Th isotopes except by radioactivity). We think that this condition is not met in our samples, thus preventing the obtaining of reliable ages. In fact, our samples show clear evidence that a recrystallization process has occurred. This indicates a potential opening of the radioactive system and this opening will essentially affect the uranium isotopes that can be transferred without necessarily fractionation of ^{234}U-^{238}U. Deschamps et al. (2004) observed a disequilibrium of ^{234}U/^{238}U in Mesozoic

Table. U series dating results of the Milet Formation.

Sample no.	Depth (m)	^{238}U ppb	±	^{232}Th ppb	±	^{234}U/^{238}U	±	^{230}Th/^{238}U	±	^{230}Th/^{232}Th	±	Calculated age (ka)	±	Corrected age (ka)	±
1	0	269.6533	1.1178	36.8952	0.1989	1.1552	0.0046	1.2187	0.0062	27.2212	0.2157	660.642	208.165	659.008	302.898
2	10	500.2964	1.6345	99.2053	0.5479	1.2591	0.0053	1.3242	0.0045	20.4088	0.1311	412.043	21.847	407.576	49.450
3	12	578.2602	2.6088	126.2914	0.7374	1.0267	0.0039	1.0347	0.0098	14.4791	0.1681	626.523	329.080	618.916	450.035
4	24	238.8013	1.6988	453.7210	6.5519	1.0653	0.0082	1.0879	0.0078	1.7499	0.0277	593.702	259.120	538.797	2249.599
5	30	535.9998	1.9015	179.0017	1.3190	1.0460	0.0042	1.0355	0.0040	9.4761	0.0797	399.761	25.644	389.269	62.890
6	36.5	729.7777	3.0307	270.3427	2.5858	1.0199	0.0049	1.0299	0.0073	8.4972	0.0998	Older than 600 ka	n.d.	Older than 600 ka	n.d.
7	57	714.4085	3.3484	41.2162	0.2128	1.0640	0.0044	1.0402	0.0065	55.1063	0.4795	346.162	19.108	343.372	19.934
8	70.5	148.2832	0.8005	2.6312	0.0136	1.0940	0.0065	1.0931	0.0067	188.2735	1.6321	380.554	30.516	378.758	30.541

limestone formations in the eastern Paris basin and they suggested discrete uranium mobility/transfer as a result of pressure dissolution structures (stylolites or dissolution of seams). The uranium mobility/transfer mechanism can be evoked to induce the slight disequilibrium observed in our samples. On the other hand, and given the old ages of the travertines, the U series activity ratios should be near the secular equilibrium (limit of the method: 500–600 ka). Thus, any small mobility or transfer of uranium will result in huge differences in the calculated ages due to the exponential character of the radioactivity phenomena. The precision of the dating decreases with increasing age (Geyh and Schleicher, 1990 and references therein).

Whatever the process responsible for the disequilibrium observed in our samples, and given the limited number of analyzed samples, we suggest that from a theoretical point of view the samples that lost a part of their uranium will yield calculated ages older than the true age, while those that gained uranium will yield a younger age than the true one. From this perspective, one can consider that the youngest calculated age (~346 ± 19 ka) can be considered as a minimum age for this formation.

Consequently, the lacustrine carbonates of the Milet Formation were deposited in the Middle Pleistocene, most likely until ~346 ka (Table).

4.3.2. Göktepe fault

The Göktepe fault is a 6-km-long fault that extends along the western part of the study area. The fault is an eastward dipping high angle normal fault that strikes towards the northwest (Figures 1b and 10). The Göktepe normal fault is divided into two segments; each of them is approximately 2 km long and extends toward the north. These branches separate the Mio-Pleistocene sedimentary units from the metamorphic basement. This fault shows a growth fault geometry because the thickness of the sequences on the footwall block is distinctly thicker than those on the hanging wall block. The Millet Formation is highly inclined due to fault dragging to the north of Göktepe village. However, the uppermost levels of the Milet Formation overlap the Göktepe fault (Figures 10 and 11). Our field observations show that the limestone beds in the upper part of the formation are undisturbed at elevations of ~800 m. This location is shown with a red square in Figure 1b. Our U/Th dating results of the uppermost levels of the travertine-type lacustrine carbonates (Milet Formation) yield a minimum radiometric age of ~346 ka B.P. (Middle Pleistocene). Since these carbonates overlapped the Göktepe fault, it may imply that this fault has been not active since at least ~346 ka (Figure 11).

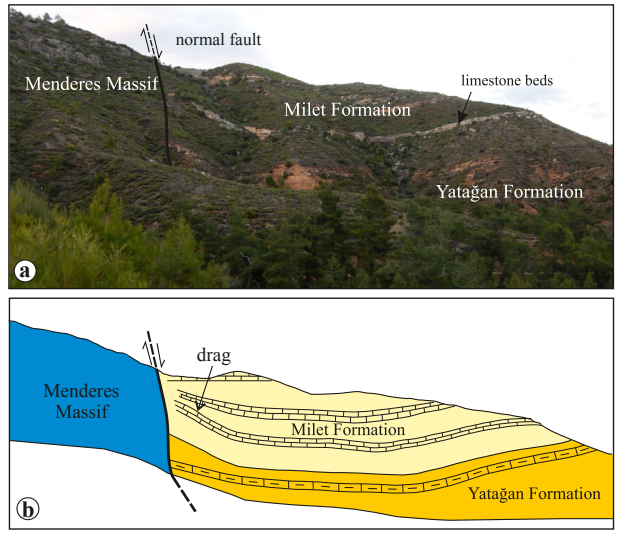

Figure 10. Photograph and drawing to show the northern branch of the 2-km-long, NW-SE trending Göktepe fault. The drag of limestone beds along the fault zone indicates a normal sense of movement. This normal fault put Mio-Pleistocene sedimentary units up against a metamorphic basement that is composed of marble and mica-schist.

4.4. Paleoenvironmental evolution

Our stratigraphic, biostratigraphic, and structural data provide a basis to evaluate the depositional environment and the climatic conditions of i) late early Miocene–early middle Miocene, ii) middle–late middle Miocene, and iii) Middle Pleistocene terrestrial deposits, which have implications for the paleoenvironmental and tectonic evolution of the Göktepe area.

4.4.1. Late Early Miocene–Early Middle Miocene (MN4–5)

The oldest deposits of the study area are fluvial clastics (alternation of conglomerates, sandstones, and mudstones) with some lacustrine interbeds (claystone, carbonated mudstone, and marl). These lacustrine layers include some gastropod fossils, Sungur palynomorph assemblages, mammalian bones, and a mandible, which provide an age constraint of late early–early middle Miocene (MN4–5). Additionally, the gastropods and palynomorph assemblages indicate a lacustrine environment that was surrounded by broad-leaved, deciduous forests under a warm subtropical climate. Some of the palynomorphs (e.g., *Botroyococcus*, *Acacia*, *Calamus*, and *Anemia*) and gastropods tolerant to brackish conditions suggest that this lake may have had brackish characteristics.

The late early–early middle Miocene (Burdigalian (20.44 Ma)–Langhian (13.82 Ma), MN4–5) corresponds to the deposition period of the lower part of the Turgut Formation in the Yatağan Basin, which should chronologically correspond with the Eskihisar and the lower part of the Yeni-Eskihisar sporomorph associations (Benda and Meulenkamp, 1990). Studies on the base of the Turgut Formation are very limited and most studies attribute a middle Miocene age for the formation (Atalay,

1980; Akgün and Sözbilir, 2001). However, Alçiçek (2010 in fig. 2 and fig. 3) suggested an early to middle Miocene (MN4–6) age for the Turgut Formation by using fossil findings of mollusks by Becker-Platen (1970) and vertebrates by Saraç (2003). Our results provide the age constraint of MN4–5 for the deposition time of the lower part of the Turgut Formation.

The early Miocene succession in the Kale-Tavas Basin consists of the Yenidere, Künar, and Kale formations (Hakyemez, 1989) (Figure 2). Among these formations, the age of the Künar Formation is the least constrained because it lacks any paleontological findings. Hakyemez (1989) considered the Künar Formation as the fluvial continental equivalent of the marine Kale Formation and therefore suggested its age as Burdigalian. Özcan et al. (2009) described two foraminiferal horizons in the middle part of the Kale Formation and indicated a transgression referring to the Burdigalian age. Büyükmeriç (2017) used stratigraphic relations between the Aquitanian Yenidere Formation and late Burdigalian Kale Formation and proposed the age of the Künar Formation as early Burdigalian. Büyükmeriç (2017) also stated that in the late Burdigalian there was a transgression in the Kale-Tavas Basin characterized by the thick carbonate sequence of the Kale Formation. Moreover, De Graciansky (1972) proposed that a branch of the early Miocene Neotethys Ocean extended towards the Kemer barrage, i.e. the Göktepe area (Figure 12). This transgression may have affected the deposition of the Turgut Formation in the Göktepe area and would explain the existence of the brackish-tolerant palynomorph assemblage and gastropods.

When the lower part of the Turgut Formation started to deposit in the Yatağan Basin, the Künar/Kale formations were deposited in the Kale-Tavas Basin (Akgün and Sözbilir, 2002) and the Kultak Formation was deposited in the Ören Basin (Kayseri-Özer et al, 2014).

4.4.2. Middle–Late Middle Miocene (MN6–7)

The middle Miocene period is characterized by fluvial and lacustrine sediments of the Turgut and Sekköy formations. The debated stratigraphic setting of the coal (lignite) in the Yatağan Basin was described in Section 1. Our fossil findings (mammalian bones, ostracods, and Çamoluk palynomorph assemblage correlated with the upper part of the Eskihisar and Yeni-Eskihisar palynomorph associations (Benda and Meulenkamp, 1990)) show that the lignite was deposited during the middle–late middle Miocene (MN6–7) time interval in the freshwater lacustrine environment. Coal-bearing sediments of the Turgut Formation were deposited under warm temperate climatic conditions. It could be said that cooling in the palaeoclimatic conditions (from subtropical to warm temperate) is observed during the deposition of the Turgut Formation in the study area (Benda and Meulenkamp, 1990). Hence, the lignite

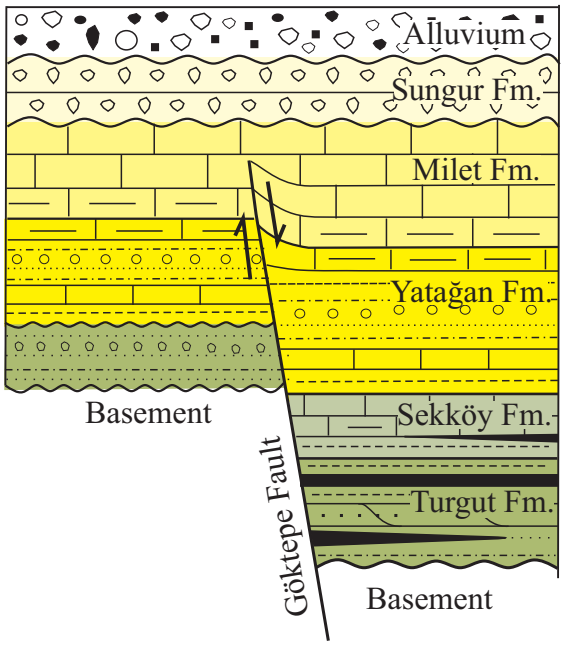

Figure 11. Asymmetry in the basin fill indicates that the Göktepe fault was a growth fault. The formations in the hanging wall are several times thicker than those in the footwall.

stratigraphically forms the uppermost levels of the Turgut Formation as proposed by Atalay (1980) and is followed by the marls of the Sekköy Formation (Bouchal et al., 2017; Güner et al., 2017).

4.4.3. Middle Pleistocene

The Göktepe area is also located in the south of the Bozdoğan Graben. The N-S running Bozdoğan Graben is a product of E-W extension before the late Miocene (Ocakoğlu et al., 2014). The NW-SE striking Göktepe fault lies at the southeastern end of the graben and may therefore be related to this extension. Moreover, the fault appears to be extinct by ~364 ka (Middle Pleistocene), which is compatible with the direction change of the extension in the Early Pliocene to the NE-SW, and then to N-S extension in the Late Pliocene-Quaternary (Ocakoğlu et al., 2014).

4.5. Conclusions

The preceding description of the stratigraphy and biostratigraphy allows evaluating the paleoenvironmental conditions in the basin. The fossil evidence of the late early to early middle Miocene indicates a warm, subtropical brackish/freshwater lacustrine environment that was surrounded by broad-leaved deciduous forests that were poor in diversity but rich in conifers. The lacustrine condition implies a transgression caused by tectonic subsidence in the basin. In the case of a brackish lake, the saline conditions could be explained by a marine

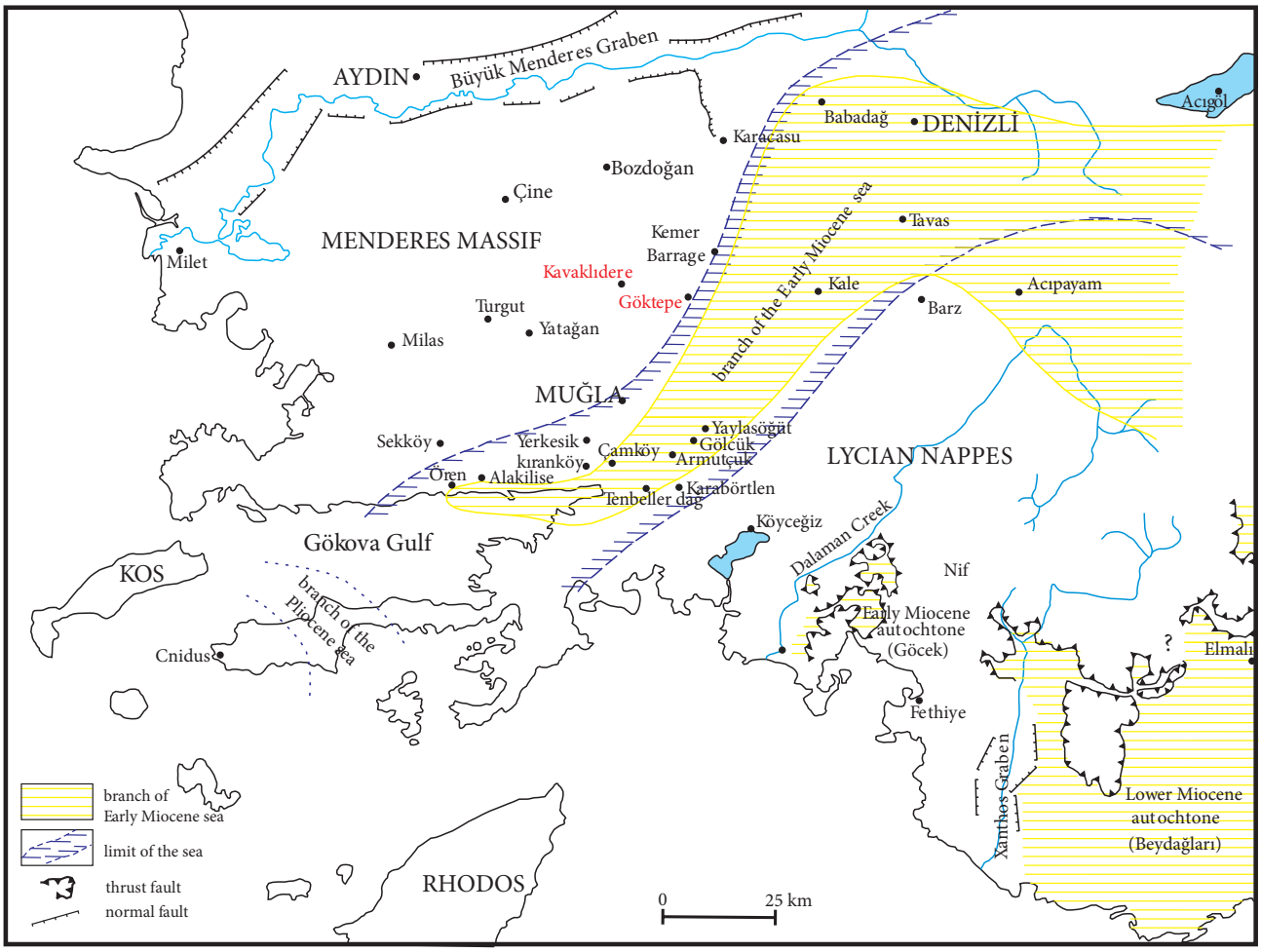

Figure 12. The map showing the extension of the early Miocene Sea (redrawn and modified after De Graciansky, 1972).

transgression. The fossil record of the middle-late middle Miocene lignite deposits presents a freshwater lacustrine environment under warm temperate climatic conditions. The sedimentary sequences on the hanging-wall block of the Göktepe fault are significantly thicker than those on the footwall block. This may indicate continuous subsidence in the basin until ~364 ka.

Acknowledgments

This study was carried out as a PhD thesis at Dokuz Eylül University and was funded by the university's BAP research unit (Project Number: 2014 KB FEN 026). We are very grateful to Bassam Ghaleb for helping to interpret the U/Th analysis results and we also appreciate the reviewers for their constructive comments.

References

Akgün F (2002). Stratigraphic and paleoenvironmental significance of Eocene palynomorphs of the Çorum-Amasya Area in the Central Anatolia, Turkey. Acta Palaeontologica Sinica 41: 576-591.

Akgün F, Akay E, Erdoğan B (2002). Terrestrial to shallow marine deposition in Central Anatolia: a palynological approach. Turkish Journal of Earth Sciences 11: 1-27.

Akgün F, Akkiraz MS, Üçbaş SD, Bozcu M, Kapan Yeşilyurt S et al. (2013). Oligocene vegetation and climate characteristics in north-west Turkey: Data from the South-western part of the Thrace Basin. Turkish Journal of Earth Sciences 22: 277-303. doi: 10.3906/yer-1201-3

Akgün F, Akyol E (1999). Palynostratigraphy of the coal-bearing Neogene deposits graben in Büyük Menderes Western Anatolia. Geobios 32: 367-383.

Akgün F, Kayseri MS, Akkiraz MS (2007). Paleoclimatic evolution and vegetational changes during the Late Oligocene–Miocene period in Western and Central Anatolia (Turkey). Palaeogeography, Palaeoclimatology, Palaeoecology 253: 56-90. doi: 10.1016/j.palaeo.2007.03.034

Akgün F, Olgun E, Kuşçu İ, Toprak V, Göncüoğlu MC (1995). Orta Anadolu kristalen kompleksinin "Oligo-Miyosen" örtüsünün stratigrafisi, çökelme ortamı ve gerçek yaşına ilişkin yeni bulgular. Turkish Association of Petroleum Geologists Bulletin 6: 51-68 (in Turkish with English abstract).

Akgün F, Sözbilir H (2001). A palynostratigraphic approach to the SW Anatolian molasse basin: Kale–Tavas molasse and Denizli molasse. Geodinamica Acta 14: 71-93. doi: 10.1016/S0985-3111(00)01054-8

Akkiraz MS, Akgün F, Örçen S (2011). Stratigraphy and palaeoenvironment of the lower-"middle" Oligocene units in the northern part of the Western Taurides (İncesu area, Isparta, Turkey). Journal of Asian Earth Sciences 40: 452-474. doi: 10.1016/j.jseaes.2010.09.010

Akkiraz MS, Kayseri MS, Akgün F (2008). Palaeoecology of coal-bearing Eocene sediments in Central Anatolia (Turkey) based on quantitative palynological data. Turkish Journal of Earth Sciences 17: 317-360.

Akyol E (1971). Microflora Oligocene collected in a survey near Avcıkoru, Şile-Istanbul. Pollen et Spores 13: 117-133 (in French with English abstract).

Alçiçek CM, ten Veen JH (2008). The late Early Miocene Acıpayam piggy-back basin: Refining the last stages of Lycian nappe emplacement in SW Turkey. Sedimentary Geology 208: 101-113. doi: 10.1016/j.sedgeo.2008.05.003

Alçiçek H (2010). Stratigraphic correlation of the Neogene basins in southwestern Anatolia: regional palaeogeographical, paleoclimatic and tectonic implications. Palaeogeography, Palaeoclimatology, Palaeoecology 291: 297-318. doi: 10.1016/j.palaeo.2010.03.002

Atalay Z (1980). Muğla - Yatağan ve yakın dolayı karasal Neojen'inin stratigrafi araştırması. Türkiye Jeoloji Kurumu Bülteni 23: 93-99 (in Turkish with English abstract).

Batı Z, Sancay RH (2007). Palynostratigraphy of Rupelian sediments in the Muş Basin, Eastern Anatolia, Turkey. Micropaleontology 53: 244-283. doi: 10.2113/gsmicropal.53.4.249

Batten DJ (1999). Small palynomorphs. In: Jones TP, Rowe NP (editors). Fossil Plants and Spores: Modern Techniques. London, UK: Geological Society, pp. 15-19.

Becker-Platen JD (1970). Lithostratigraphische Unterschungen im Kanozoikum Sudwest Anatoliens (Turkei) – Kanozoikum und Braunkohlen der Turkei. Beihhefte zum Geologischen Jahrbuch 97: 1-244 (in German with English abstract).

Benda L (1971). Grundzüge einer pollenanalytischen Gliederung des türkischen Jungtertiärs (Känozoikum und Braunkohle der Türkei. 4). Beihhefte zum Geologischen Jahrbuch 113: 1-46 (in German with English abstract).

Benda L, Muelenkamp JE (1990). Biostratigraphic correlations in the Eastern Mediterranean Neogene 9. Sporomorph associations and event stratigraphy of the Eastern Mediterranean Neogene. Newsletter Stratigraphy 23 (1): 1-10.

Bergounioux FM, Zbyszewski G, Crouzel F (1953). Les Mastodontes Miocènes de Portugal. Memoires dos Serviços Geologicos de Portugal, Lisboa, Nouvelle Serie 1: 1-140 (in Portuguese).

Bouchal JM, Mayda S, Zetter R, Grimsson F, Akgün F et al. (2017). Miocene palynofloras of the Tınaz lignite mine, Muğla, southwest Anatolia: taxonomy, paleoecology and local vegetation change. Review of Paleobotany and Palynology 243: 1-36. **doi:** 10.1016/j.revpalbo.2017.02.010

Bouchal JM, Zetter R, Grimsson F, Denk T (2016). The middle Miocene palynoflora and paleoenvironments of Eskihisar (Yatağan Basin, south-western Anatolia): a combined LM and SEM investigation. Botanical Journal of the Linnean Society 182: 14-79.

Brongniart A (1822). Sur la classification et la distribution des végétaux fossiles en général et sur ceux des terrains de sédiment supérieur en particuliére. Mémoire du Museum Nationale d'Histoire Naturelle Paris 8: 203-240 (in French).

Büyükmeriç Y (2017). Molluscan biostratigraphy of early Miocene deposits of the Kale-Tavas and Acıpayam basins (Denizli, SW Turkey). Bulletin of the Mineral Research and Exploration 155: 49-73. doi: 10.19111/bulletinmre.302166

Cavagnetto C, Anadón P (1996). Preliminary palynological data on floristic and climatic changes during the Middle Eocene-Early Oligocene of the eastern Ebro Basin, northeast Spain. Review of Palaeobotany and Palynology 92: 281-305.

Collins AS, Robertson AHF (1998). Processes of Late Cretaceous to Late Miocene episodic thrust-sheet translations in the Lycian Taurides, SW Turkey. Journal of the Geological Society of London 155: 759-772.

De Graciansky PC (1972). Recherches géologiques' dans le Taurus lycien occidental. PhD, University of Paris-Sud, Orsay, France (in French with English abstract).

Deschamps P, Hillaire-Marcel C, Michelot JL, Doucelance R, Ghaleb B et al. (2004). $^{234}U/^{238}U$ disequilibrium along stylolitic discontinuities in deep Mesozoic limestone formations of the Eastern Paris basin: evidence for discrete uranium mobility over the last 1-2 million years. Hydrology and Earth System Sciences 8 (1): 35-46.

Ediger VŞ, Batı Z, Alişan C (1990). Paleopalynology and paleoecology of Calamus-like disulcate pollen grains. Review of Paleobotany and Palynology 62: 97-105. doi: 10.1016/0034-6667(90)90019-F

Erdei B, Yavuz N, Akgün F, Hably L (2002). Some data to the Miocene flora of Western Turkey. In: 6th European Palaeobotany Palynology Conference, Athens, Abstract Book, pp. 79-80.

Erdoğan B, Güngör T (2004). The problem of the core-cover boundary of the Menderes Massif and an emplacement mechanism for regionally extensive gneissic granites, Western Anatolia (Turkey). Turkish Journal of Earth Sciences 13: 15-36.

Freels D (1980). Limnische Ostrakoden aus Jungtertiar und Quartar der Turkei. Geologisches Jahrbuch 39: 3-169 (in German with English abstract).

Fortelius M (1990). Rhinocerotidae from Paşalar, middle Miocene of Anatolia (Turkey). Journal of Human Evolution 19 (4-5): 489-508.

Geraads D, Miller E (2013). *Brachypotherium minor* n. sp., and other Rhinocerotidae from the Early Miocene of Buluk, Northern Kenya. Geodiversitas 35 (2): 359-375.

Geyh MA, Schleicher H (1990). Absolute Age Determination. Physical and Chemical Dating Methods and Their Application. Berlin, Germany: Springer. doi: 10.1007/978-3-642-74826-4

Ghaleb B, Falguères C, Carlut J, Pozzi JP, Mahieux G et al. (2019). Timing of the Brunhes-Matuyama transition constrained by U-series disequilibrium, Scientific Reports 9: 6039 doi: 10.1038/s41598-019-42567-2

Gruas-Cavagnetto C (1977). Etude palynologique de l'Eocene du Bassin Anglo–Parisien. PhD, University of Pierre Marie Curie VI, Paris, France (in French).

Güner TH, Bouchal JM, Köse N, Göktaş F, Mayda S et al. (2017). Landscape heterogeneity in the Yatağan Basin (southwestern Turkey) during the middle Miocene inferred from plant macrofossils. Palaeontographica Abteilung B 296 (1-6):113-171.

Gürer ÖF, Sangu E, Özburan M, Gürbüz A, Sarıca Filoreau N (2013). Complex basin evolution in the Gökova Region: implications on the Late Cenozoic tectonics of southwest Turkey. International Journal of Earth Science 102: 2199-222. doi: 10.1007/s00531-013-0909-1

Gürer ÖF, Yılmaz Y (2002). Geology of the Ören and surrounding areas, SW Anatolia. Turkish Journal of Earth Sciences 11: 1-13.

Hakyemez HY (1989). Kale–Kurbalık (GB Denizli) bölgesindeki Senozoyik yaşlı çökel kayaların jeolojisi ve stratigrafisi. Bulletin of the Mineral Research and Exploration 109: 9-21 (in Turkish with English abstract).

Harzhauser M, Daxner Höck G, Göhlich UB, Nagel D (2011). Complex faunal mixing in the early Pannonian palaeo-Danube Delta (Late Miocene, Gaweinstal, Lower Austria). Annalen des Naturhistorischen Museums in Wien 113 (A): 167-208.

Harzhauser M, Kowalke T, Mandic O (2002). Late Miocene (Pannonian) gastropods of Lake Pannon with special emphasis on early ontogenetic development. Annalen des Naturhistorischen Museums in Wien 103 (A): 75-141.

Harzhauser M, Mandic O (2008). Neogene lake systems of Central and South-Eastern Europe: Faunal diversity, gradients and interrelations. Palaeogeography Palaeoclimatology Palaeoecology 260: 417-434. doi: 10.1016/j.palaeo.2007.12.013

Harzhauser M, Mandic O, Büyükmeriç Y, Neubauer TA, Kadolsky D et al. (2016). A Rupelian mangrove swamp mollusc fauna from the Thrace Basin in Turkey. Archiv für Molluskenkunde 145 (1): 23-58. doi: 10.1127/arch.moll/1869-0963/145/023-058

Inaner H, Nakoman E, Karayiğit AI (2008). Coal resource estimation in the Bayir Field, Yatağan–Muğla, SW Turkey. Energy Sources Part A 30: 1000-1015. doi: 10.1080/15567030601088925

Karayiğit Aİ, Akgün F, Gayer RA, Temel A (1999). Quality, palynology, and palaeoenvironmental interpretation of the Ilgin lignite, Turkey. International Journal of Coal Geology 38: 219-236.

Kayseri MS (2010). Oligo-Miocene palynology, palaeobotany, vertebrate, marine faunas, palaeoclimatology and palaeovegetation of the Ören Basin (North of the Gökova Gulf), Western Anatolia. PhD, Dokuz Eylül University, İzmir, Turkey.

Kayseri MS, Akgün F (2008). Palynostratigraphic, palaeovegetational and palaeoclimatic investigations on the Miocene deposits in Central Anatolia (Çorum Region and Sivas Basin). Turkish Journal of Earth Sciences 17: 361-403.

Kayseri-Özer MS (2014). Spatial distribution of climatic conditions from the Middle Eocene to Late Miocene based on palynoflora in Central, Eastern and Western Anatolia. Geodinamica Acta 26 (1-2): 122-157.

Kayseri-Özer MS, Akgün F, Mayda S, Kaya T (2014). Palynofloras and vertebrates from Muğla-Ören region (SW Turkey) and palaeoclimate of the Middle Burdigalian–Langhian period in Turkey. Bulletin of Geosciences 89: 137-162. doi: 10.3140/bull.geosci.1407

Koçyiğit A (1984). Güneybatı Türkiye ve yakın dolayında levha içi yeni tektonik gelişim. Türkiye Jeoloji Kurumu Bülteni 27: 1-17 (in Turkish with English abstract).

Konak N, Akdeniz N, Öztürk EN (1987). Geology of the South of Menderes Massif. IGCP Proj. 5: Guide Book Field Excursion Western Anatolia, Turkey. Ankara, Turkey: Mineral Research and Exploration Institute of Turkey.

Ludwig KR (2012). User's Manual for Isoplot 3.75, A Geochronological Toolkit for Microsoft Excel, Vol. 5. Berkeley, CA, USA: Berkeley Geochronology Center Special Publications.

Ludwig KR, Paces JB (2002). Uranium-series dating of pedogenic silica and carbonate, Crater Flat, Nevada. Geochimica et Cosmochimica Acta 66 (3): 487-506.

Maldonado E, Mazo AV, Alferez F (1983). Los mastodontes (Proboscidea, Mammalia) del Orleaniense medio de Corcoles (Guadalajara). Estudios Geologicos (Madrid) 39 (5-6): 431-449 (in Spanish with English abstract).

Markov GN, Vergiev S (2010). First report of cf. *Protanancus* (Mammalia, Proboscidea, Amebelodontidae) from Europe. Geodiversitas 32 (3): 493-500. doi: 10.5252/g2010n3a6

Matheron P (1843). Catalogue méthodique et descriptif des corps organisés fossiles du département des Bouches-du-Rhône et lieux circonvoisins précedé d'un Mémoire sur les terrains supérieurs au grès bigarré du S.E. de la France. Répertoire des travaux de la Société de Statistique de Marseille 6: 81-341 (in French).

Matzke-Karasz R, Witt W (2005). Ostracods of the Paratethyan Neogene Kılıç and Yalakdere formations near Yalova (İzmit Province, Turkey). Zitteliana A (45): 115-133.

Mikuz V, Pavsic J (2000). *Brotia* (*Tinnyea*) *escheri* (Brongniart) iz miocenskih plastipiri tunjicah (*Brotia* (*Tinnyea*) *escheri* (Brongniart) from Miocene beds at Tunjice, Central Slovenia). Geologija 43 (1): 43-53.

Mazo AV (1977). Revision de los mastodontes de España. PhD, Universidad Complutense, Madrid, Spain (in Spanish).

Mazo AV (1996). Gomphotheres and Mammutids from the Iberian Peninsula. In: Shoshani J, Tassy P (editors). The Proboscidea. Evolution and Palaeoecology of Elephants and Their Relatives. New York, NY, USA: Oxford University Press, pp. 136-142.

Nakoman E (1966). Palynological contribution of Tertiary formations in the Thrace Basin. I. Qualitative study. Annales de la Société Géologique du Nord 86: 65-107.

Nakoman E (1978). Linyit içeren Soma Neojen bölgesi. Batı Anadolu. Maden Tetkik Arama Enstitüsü Dergisi 90: 20-70 8 (in Turkish).

Nakoman E, İnaner H (1996). Turgut Bayır ve Karacahisar Linyit Sektörlerinin Ekonomik Jeoloji Yönünden Değerlendirilmesi, Scientific Project, No: 0908-95-06-04. İzmir, Turkey: Dokuz Eylül University (in Turkish).

Nebert K (1956). Denizli–Acıgöl Merkezinin Jeolojisi, 1/100.000 Ölçekli Denizli 105/1, 105/2 ve Isparta 106/1 Paftalarının Sahası İçinde Yapılan Jeolojik Harita Çalışmaları Hakkında Rapor. Mineral Research and Exploration Institute (MTA), Report No: 2509. Ankara, Turkey: MTA (in Turkish).

Ocakoğlu F, Açıkalın S, Özsayın E, Dirik RK (2014). Tectonosedimentary evolution of the Karacasu and Bozdoğan basins in the Central Menderes Massif, W Anatolia. Turkish Journal of Earth Sciences 23: 361-385. doi: 10.3906/yer-1309-12

Okay AI (2001). Stratigraphic and metamorphic inversions in the central Menderes Massif: a new structural model. International Journal of Earth Sciences 89: 709-727. doi: 10.1007/s005310000098

Önay TŞ (1949). Über die Smirgelgesteine Südwest-Anatoliens. Schweizerische Mineralogische und Petrographische Mitteilungen 29: 357-491 (in German).

Özcan E, Less G, Beke-Baldi M, Kollanyi K, Acar F (2009). Oligo-Miocene foraminiferal record (Miogypsinidae, Lepidocyclinidae and Nummulitidae) from the Western Taurides (SW Turkey): biometry and implications for the regional geology. Journal of Asian Earth Science 34: 740-760. doi: 0.1016/j.jseaes.2008.11.002

Özer S, Sözbilir H (2003). Presence and tectonic significance of Cretaceous rudist species in the so-called Permo-Carboniferous Göktepe Formation, central Menderes Massif, western Turkey. International Journal of Earth Sciences 92: 397-404. doi: 10.1007/s00531-003-0333-z

Pickford M (2001). Intérêt biochronologique des Kubanochoerinae (Mammalia, Suidae) et étude de nouveaux restes de *Megalochoerus khinzikebirus* et *Libycochoerus massai* du Kenya. Comptes Rendus de l'Académie des Sciences Series IIA 332: 193-200 (in French with English abstract).

Pickford M, Ertürk C (1979). Suidae and Tayassuidae from Turkey. Bulletin of the Geological Society of Turkey 22: 141-154.

Pickford M, Morales J (2003). New Listriodontinae (Mammalia, Suidae) from Europe and a review of listriodont evolution, biostratigraphy and biogeography. Geodiversitas 25 (2): 347-404.

Plaziat JC, Cavagnetto C, Koeniguer JC, Baltzer F (2001). History and biogeography of the mangrove ecosystem, based on a critical reassessment of the paleontological record. Wetlands Ecology and Management 9: 161-179.

Querol X, Alastuey A, Plana F, Lopez Soler A, Tuncali E et al. (1999). Coal geology and coal quality of the Miocene Mugla Basin, southwestern Anatolia, Turkey. International Journal of Coal Geology 41: 311-332.

Riegel W, Bode T, Hammer J, Hammer-Schiemann G, Lenz O et al. (1999). The palaeoecology of the Lower and Middle Eocene at Helmstedt, Northern Germany-A study in contrasts. Acta Palaeobotanica Supplement 2: 349-358.

Ring U, Johnson C, Hetzel R, Gessner K (2003). Tectonic denudation of a Late Cretaceous-Tertiary collisional belt-regionally symmetric cooling patterns and their relation to extensional faults in the Anatolide belt of western Turkey. Geological Magazine 140: 1-21.

Sancay RH, Batı Z, Işık U, Kırıcı S, Akça N (2006). Palynomorph, foraminifera, and calcareous nanoplankton biostratigraphy of Oligo–Miocene sediments in the Muş Basin, Eastern Anatolia, Turkey. Turkish Journal of Earth Sciences 15: 259-319.

Saraç G (2003). Mammal Fossil Findings in Turkey. Scientific Report No: 10609208p. Ankara, Turkey: MTA (in Turkish).

Seyitoğlu G, Işık V (2015). Late Cenozoic extensional tectonics in Western Anatolia: exhumation of the Menderes core complex and formation of related basins. Bulletin of the Mineral Research Exploration 151: 47-106.

Seyitoğlu G, Işık V, Çemen İ (2004). Complete Tertiary exhumation history of the Menderes Massif, western Turkey: an alternative working hypothesis. Terra Nova 16: 358-363.

Seyitoğlu G, Scott B (1991). Late Cenozoic crustal extension and basin formation in west Turkey. Geological Magazine 128: 155-166.

Sözbilir H (2005). Oligo-Miocene extension in the Lycian Orogen: evidence from the Lycian molasse basin, SW Turkey. Geodinamica Acta 18: 255-282. doi: 10.3166/ga.18.255-282

Şengör AMC, Yılmaz Y (1981). Tethyan evolution of Turkey: a plate tectonic approach. Tectonophysics 75: 181-241.

Tassy P (1985). La place des mastodontes miocènes de l'Ancien Monde dans la phylogénie des Proboscidea (Mammalia): hypothèses et conjectures. Thèse Dr. ès Sc. Mémoires des Sciences de la Terre Université Curie Paris. Paris, France: Pierre and Marie Curie University (in French)

Tassy P (2014). L'odontologie de *Gomphotherium angustidens* (Cuvier, 1817) (Proboscidea, Mammalia): données issues du gisement d'En Péjouan (Miocène moyen du Gers, France). Geodiversitas 36 (1): 35-115 (in French with English abstract).

Ten Veen JH, Boulton SJ, Alçiçek MC (2009). From palaeotectonics to neotectonics in the Neotethys realm: the importance of kinematic decoupling and inherited structural grain in SW Anatolia (Turkey). Tectonophysics 473: 261-281. doi: 10.1016/j.tecto.2008.09.030

Ünal D (1988). Geology of Muğla-Milas-Ören-Alatepe Fields; Report No: KÖ 86. Ankara, Turkey: Mineral Research and Exploration Institute (in Turkish).

Van Der Made J (1996). Listriodontinae (Suidae, Mammalia), their evolution, systematics and distribution in time and space. Contributions to Tertiary and Quaternary Geology 33: 3-254.

Van Morkhoven FPCM (1963). Post-paleozoic Ostracoda. Their Morphology, Taxonomy and Economic Use. Amsterdam, the Netherlands: Elsevier.

Witt W (2003). Freshwater ostracods from Neogene deposits of Develiköy (Manisa Turkey). Zittelina A 43: 93-108.

Yılmaz Ö, İşintek İ, Kayseri-Özer MS, Güngör T (2016). Correlation of microfacies changes and stable isotope values on travertine type carbonates: a case study of Göktepe (Mugla)-Preliminary results. In: 7th Quaternary Symposium of Turkey, Symposium Proceedings, p. 154.

Yılmaz Y, Genç SC, Gürer OF, Bozcu M, Yılmaz K et al. (2000) When did the western Anatolian grabens begin to develop? In: Bozkurt E, Winchester JA, Piper JDA (editors). Tectonics and Magmatism in Turkey and the Surrounding Area. London, UK: Geological Society of London Special Publications, pp. 353-384.